

Research Article

Impact of Combined Acidic and Hyperosmotic Shock Conditions on the Proteome of *Listeria monocytogenes* ATCC 19115 in a Time-Course Study

Dong Lai Zhang¹,¹ Ya Long Bai,¹ and John P. Bowman²

¹Institute of Agri-Food Standards and Testing Technology, Shanghai Key Laboratory of Protected Horticultural Technology, Shanghai Academy of Agricultural Sciences, 1000 Jinqi Road, Shanghai, China

²Food Safety Centre, Tasmanian Institute of Agriculture, University of Tasmania, Hobart, Tasmania, Australia

Correspondence should be addressed to Dong Lai Zhang; zhangdl2156256@hotmail.com

Received 20 June 2018; Revised 27 October 2018; Accepted 13 November 2018; Published 24 April 2019

Academic Editor: Efsthios Giaouris

Copyright © 2019 Dong Lai Zhang et al. This is an open access article distributed under the Creative Commons Attribution License, which permits unrestricted use, distribution, and reproduction in any medium, provided the original work is properly cited.

Listeria monocytogenes can cause listeriosis in humans through consumption of contaminated food and can adapt to and grow under a wide array of physiochemical stresses. Consequently, it causes persistent food safety issues and requires vigilant sanitation processes to be in place, especially for the manufacture of high-risk food products. In this study, the global proteomic responses of the food-borne pathogen *L. monocytogenes* strain ATCC 19115 were determined when exposed to nonthermal inactivation. This process was examined in the early stationary growth phase with the strain placed under simultaneous exposure to low pH (pH 3.5) and high salinity (a_w 0.900, 14% NaCl). Proteomic responses, measured using iTRAQ techniques, were conducted over a time course (5 min, 30 min, and 1 h at 25°C). The enumeration results showed that, at 5 min, cells underwent initial rapid inactivation by 1.2 log units and 2.5 log units after 30 min, and after that, culturability remained stable when sampled at 1 h. From the iTRAQ results, the proteome level changes that occur rapidly during the inactivation process mainly affected prophage, cell defense/detoxification, carbohydrate-related metabolism, transporter proteins, phosphotransferase systems, cell wall biogenesis, and specific cell surface proteins. Pathway map analysis revealed that several pathways are affected including pentose and glucuronate interconversions, glycolysis/gluconeogenesis, pyruvate metabolism, valine, leucine and isoleucine biosynthesis, oxidative phosphorylation, and proteins associated with bacterial invasion of epithelial cells and host survival. Proteome profiling provided a better understanding of the physiological responses of this pathogen to adapt to lethal nonthermal environments and indicates the need to improve food processing and storage methods, especially for non- or minimally thermally processed foods.

1. Introduction

As a potentially fatal food-borne pathogen, the Gram-positive bacterial species *Listeria monocytogenes* represents a public health threat and a burden for the food industry. This pathogen is known for its ability to survive harsh environments for instance nongrowth permissive acidic and hyperosmotic conditions, including the mild fermentation-based preservation processes used for many low pH and high salinity foods, such as fermented meat and cheese [1]. *L. monocytogenes* infections (listeriosis) can lead to gastroenteritis, meningitis, encephalitis, premature abortion, and

septicemia in susceptible individuals with a mortality rate of approximately 20% [2, 3].

Proteomics strategies have been applied to better understand the mechanisms of how *L. monocytogenes* responds to acidic, salt, cold, heat, alkali, detergent, and redox stresses, respectively [4–11]. Since the process of cells response to stresses is complex, proteomic profiles through iTRAQ techniques monitoring relative changes in protein abundance can potentially provide useful information about cellular functionality and manifested phenotypes. The response to acid and/or salt stress mainly affects the biochemical processes related to oxidative stress, nutrient

uptake, and transcriptional regulation [5, 7, 8, 12]. Knowing to what extent proteins are formed and how they merge to constitute a functional unit in response to environmental stress also provides relevant information to understanding how an organism responds to different scenarios, especially when presented against temporal scales and specific physiological contexts. Additionally, the metabolism of pathogens in response to stress can be better understood through reconstruction of metabolic pathways and understanding formation of de novo end-products, such as lipids, proteins, and metabolic intermediates. Stress-associated proteins participate in diverse cellular activities, including gene regulation, changes to intermediary metabolism, compatible solute uptake and/or synthesis, protein folding, ATP-dependent proteolysis, and DNA repair [13]. Furthermore, proteomics analysis has also shown that acclimation of *L. monocytogenes* to high but still growth permissive temperatures induces cross-protection to high salt concentrations [14]. Proteins involved in maintenance of the cell wall and amino acid metabolism, such as osmolyte transporters and lipid biosynthesis proteins, attain the greatest expression when cells are exposed to elevated temperatures prior to salt stress [14].

Multiple stresses typically occur in the food processing and preservation environments, such as combinations of low pH and high salt concentrations [15]. When boiling or chilling is not available to make food safe, such as salami and cheese products, other hurdles are required in order to improve product safety, such as the addition of acid and salt. When the main hurdles to growth or survival of pathogenic bacteria in food are nonthermal (typically pH and water activity), the main factor governing food safety during the processing and storage is temperature [16, 17].

In the present study, we aimed to identify differentially expressed proteins over a range of different sampling times (5, 30, and 60 min), using iTRAQ techniques with the objective of acquiring new and confirming existing insights into the cellular response strategy developed by *L. monocytogenes* to survive in nongrowth permissive low pH and high-salinity stress conditions. In the previous studies, we observed mRNA is stabilized in inactivated cells [18]. This suggests there may be a short window of time for protein synthesis to aid survival of cells. Prior experiments have revealed a subpopulation of cells that survive (0.01–1%) with the proportion increasing with temperature and showing longer survival time in a classic Weibull-type relationship [18]. However, the underlying physiological reasons for this survival remain unclear. Therefore, knowing how *L. monocytogenes* mechanistically responds to multiple stresses might enable the development of innovative food safety strategies for controlling listerial contamination especially in high-risk foods, such as those with minimal thermal processing and which tend to be stored for prolonged times at chill temperatures.

2. Materials and Methods

2.1. Bacterial Cultivation and Acid pH/Hyperosmotic NaCl Inactivation. *L. monocytogenes* strain ATCC 19115 (ATCC,

USA) was used in the study as it has been genome sequenced and is often used as a quality control standard strain for *Listeria monocytogenes* in food-related testing. ATCC 19115 was routinely grown using tryptone soya broth supplemented with 0.6% yeast extract (TSB-YE, Oxoid, Beijing, China) at 25°C. The acidic (pH 3.5) and hyperosmotic NaCl ($a_w = 0.90$, 14%) inactivation conditions applied to strains ATCC 19115 lie beyond and at growth permissive limits [17], respectively. For inactivation, sterile TSB-YE broth containing 2.5 M NaCl (Sigma, Shanghai, China) was adjusted to pH 3.5 using a known amount of filter-sterilized HCl. For inactivation treatments, strains were grown to the early stationary growth phase (12 h incubation at 25°C in a shaking water bath, 100 rpm) in 1 L TSB-YE broth; cultures were pelleted by centrifugation (10,000 g at 4°C for 10 min) as T0, and then cell pellets were resuspended in an equal volume of TSB-YE (pH 3.5, 2.5 M NaCl) broth and vortexed to disperse cells evenly at only one temperature of 25°C and sampling at 5 min, 30 min, and 1 hr, and plate counting using Brain-Heart Infusion (BHI) agar was supplemented with 0.1% pyruvate (BHA-P) to determine culturable cell populations. At least 100 ml of samples were taken for each proteomics experiment in order to have enough biomass for proteins analysis. Differentially expressed proteins at these time points were analyzed in comparison to the starting time point (T0). The experiments were done in triplicate.

2.2. Protein Extraction. We followed the method of Zhu et al. [19] that 1 g of wet weight of cell pellets from each of the samples (which included three independent biological replicates) was washed with phosphate buffer saline PBS (pH 7.4) to move flocculent precipitation, and then the sample was solubilized in 1/10 volumes of the SDT buffer (4% SDS, 100 mM DTT, and 150 mM Tris-HCl at pH 8.0). After 3 min incubation in boiling water, the suspensions were ultrasonicated in 10 rounds of 80 W sonication for 10 s with 15 s interval. The crude extract was clarified by centrifugation at 13,000 g at 20°C for 15 min. The protein concentration was determined using the Bicinchoninic acid (BCA) Protein Assay Kit (Promega, USA), and the supernatants were stored at –80°C until further analysis.

2.3. Protein Digestion and iTRAQ Labeling. Protein digestion was performed according to the filter-aided sample processing (FASP) procedure which was described previously [20]. In brief, 200 µg of proteins from each sample were incorporated into 30 µl of SDT buffer (4% SDS, 100 mM DTT, and 150 mM Tris-HCl at pH 8.0). Through repeated ultrafiltration (Pall units, 10 kD), the detergent, DTT, and other low-molecular-weight components were removed using UA buffer (8 M urea, 150 mM Tris-HCl at pH 8.0). After addition of 100 µL iodoacetamide (50 mM in UA) and oscillation for 1 min at 600 rpm, the samples were incubated for 30 min in darkness and then centrifuged at 13,000×g for 10 min. The filters were washed thrice with 100 µL UA buffer and twice with 100 µL DS buffer (50 mM triethylammoniumbicarbonate at pH 8.5). The protein suspensions were digested with 2 µg trypsin (Promega, USA)

in 40 μ l DS buffer at 37°C for 16 h, and then the resulting peptides were collected as a filtrate. Peptide concentration was determined by UV light spectral density at 280 nm based on the extinction coefficient of 1.1 of 0.1% (g/l) solution.

The resulting peptide was labeled using the 4-plex iTRAQ reagent according to the manufacturer's instructions (Applied Biosystems, CA). Each iTRAQ reagent was dissolved in 70 μ l of ethanol and added to the respective peptide mixture, and the samples were then labeled as (C)-113, (T1)-114, (T2)-115, and (T3)-116 with three independent biological replicates. After incubation at room temperature for 2 h and termination of the labeling reaction, the labeled samples were then mixed and vacuum-dried.

2.4. Strong Cation Exchange (SCX) Chromatography. The labeled samples were fractionated by SCX chromatography using the AKTA Purifier system (GE Healthcare, Fairfield, CT, USA). In brief, the dried peptide mixture was reconstituted in 2 ml buffer A (10 mM KH_2PO_4 in 25% of CAN at pH 2.7) and loaded onto a PolySULFOETHYL 4.6 \times 100 mm column (5 μ m, 200 Å, PolyLC Inc., Maryland, USA). The peptides were then eluted at a flow rate of 0.9 ml/min with a gradient of 0%–10% buffer B (500 mM KCl, 10 mM KH_2PO_4 in 25% of CAN at pH 2.7) from 0 to 2 min, 10%–20% buffer B until 27 min, 20%–45% buffer B until 32 min, and 50%–100% buffer B until 37 min. The elution was monitored at 214 nm, and fractions were collected every minute for a total of 35 fractions. The collected fractions were then combined into 10 pools and desalted on C18 Cartridges (66872-U, Sigma, USA). Each fraction was vacuum freeze-dried by vacuum centrifugation and reconstituted in 40 μ l of 0.1% (v/v) trifluoroacetic acid. Finally, all samples were stored at –80°C until further analysis.

2.5. LC-MS/MS Analysis. Experiments were analyzed on a Q Exactive mass spectrometer coupled to an Easy nLC system (Thermo Fisher Scientific, Waltham, MA, USA). 6 μ l of each fraction was injected for nano LC-MS/MS analysis. The peptide (5 μ g) was loaded onto a Thermo Scientific EASY column (2 cm \times 100 mm, 5 mm C18) using an autosampler. The peptides were eluted onto an analytical Thermo Scientific EASY column (75 mm \times 100 mm, 3 mm C18) and separated with a linear gradient of buffer B (0.1% formic acid and 80% acetonitrile) at a flow rate of 250 nl/min over 60 min. Mass spectrometry data were acquired in the peptide recognition mode using the 10 most abundant precursor ions from a survey scan of 300–1800 m/z after high-energy collisional dissociation fragmentation. Dynamic exclusion duration was 50 s. Survey scans were acquired at a resolution of 70,000 at m/z 200, and resolution for HCD spectra was set to 17,500 at m/z 200. Normalized collision energy was 30 eV, and the underfill ratio was defined as 0.1%. The instrument was run with the peptide recognition mode enabled.

2.6. Sequence Database Searching and Data Analysis. Mass spectrometry raw data were searched using the MASCOT engine (Matrix Science, London, UK; version 2.2)

embedded into Proteome Discoverer 1.4 (Thermo Electron, San Jose, CA) against the UniProt *Listeria* database (268763 sequences, download at 08/08/2014) and the Decoy database. For protein identification, the following searching parameters were used: peptide mass tolerance 20 ppm, MS/MS tolerance 0.1 Da, enzyme trypsin, missed cleavage 2, fixed modification carbamidomethyl (C), iTRAQ 4-plex (K), and iTRAQ 4-plex (N-term), and variable modification oxidation (M). All reported data were based on false discovery rate (FDR) of less than 1% confidence for protein identification.

2.7. Bioinformatics. The Gene Ontology (GO) program Blast2GO (<https://www.blast2go.com/>) was used to annotate DEPs (differential expression proteins) to create histograms of GO annotation, which includes biological process, cell component, and molecular function [21, 22]. For pathway analysis, the DEPs were mapped to the terms in the KEGG [23] (Kyoto Encyclopedia of Genes and Genomes) database using the KAAS program (http://www.genome.jp/kaas-bin/kaas_main). Protein-protein interaction networks were analyzed using the publicly available program STRING (<http://string-db.org/>), and the minimum required interaction score was set to 0.400.

3. Results and Discussion

In this study, we focused on conditions that promoted rapid loss of viability but was nonthermal in nature, thus focusing the loss of viability as a collapse in cytoplasmic homeostasis. The data shown were also performed with stationary phase cells, and in that respect, standard defenses arising from the general stress response were induced when entering the stationary growth phase, such as heat shock proteins and oxidative stress management proteins are already activated. What is shown here are the more specific responses to stress above and beyond the typically made observations of stress responses. This is possible due to the relative sensitivity if conventional proteomic technique used. With that said, it should be noted that studying one strain will not capture the possible extent of responses that could occur across the full diversity of *L. monocytogenes*. As found for studies examining the effect of organic acid on cell survival and gene expression, responses can vary likely due to the differing ability to maintain cytoplasmic integrity by the cell population. This leads to the differing availability of ATP per cell and thus the capacity to elicit detectable changes in protein expression [24–28].

Previous studies have carried out proteomics analyses of *L. monocytogenes* exposed to single- or dual-stress (acid and salt) conditions [5, 7, 14, 29–36]. However, the response of the proteome of *L. monocytogenes* to simultaneous exposure to acid and salt for a time-course study had not been investigated and was therefore examined in the present study. To insure the accuracy of the information of proteomes, the cells were checked for culturability at each sampling time, as shown in Figure 1(a). For the time-course study, growth of the early stationary growth phase (mean = 7.3 log CFU/ml) *L. monocytogenes* ATCC 19115 was exposed to simultaneous

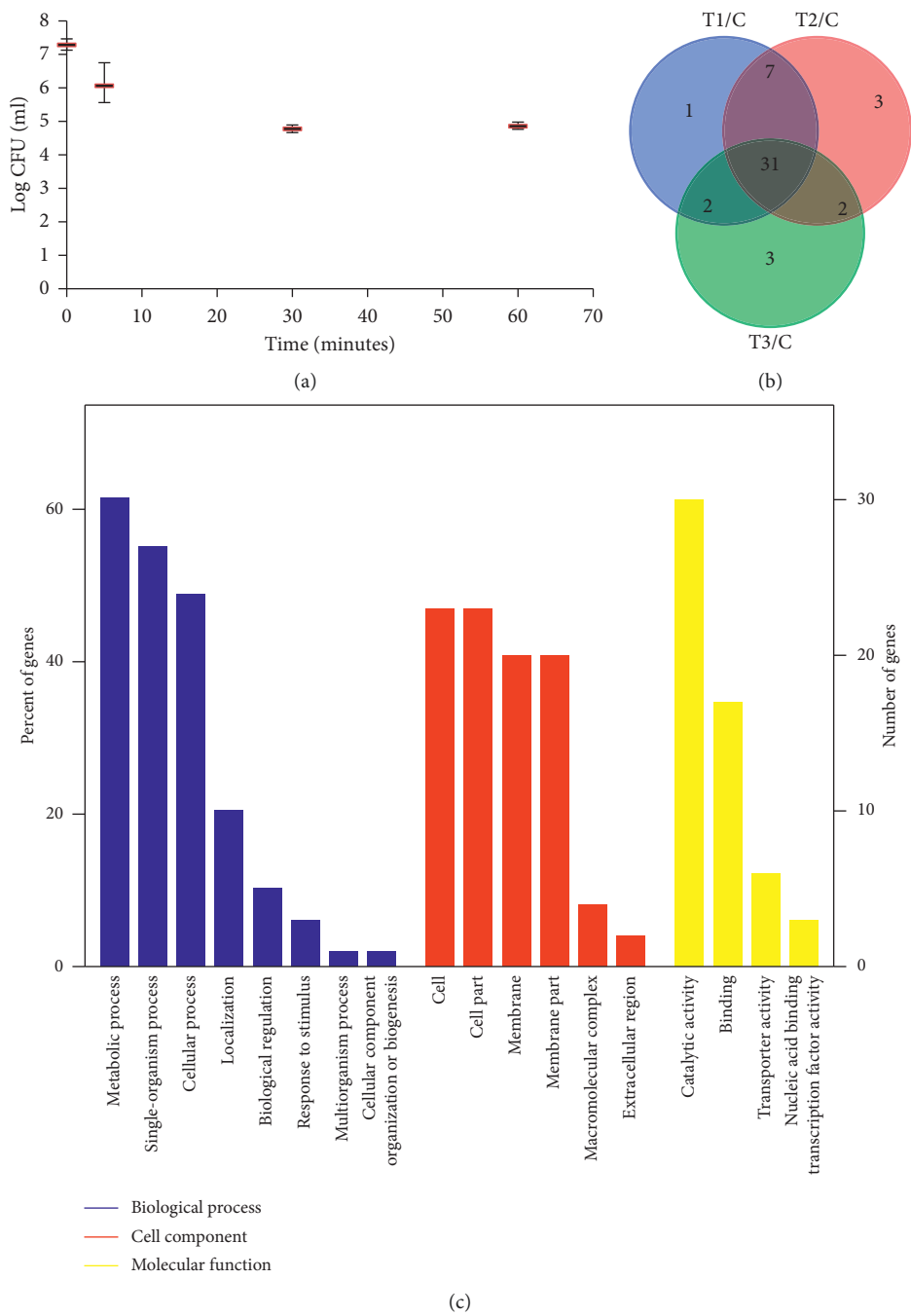


FIGURE 1: The inactivation of *L. monocytogenes* ATCC 19115 was estimated by culture-based enumeration in Tryptone Soya broth supplemented with 0.6% yeast extract (TSB-YE) with pH 3.5 (HCl as acidulant) and a_w 0.90 (NaCl as humectant). (a) Inactivation curves were constructed by plotting log CFU/ml against the sampling time of 5 min, 30 min, and 1 hr at 25°C with an initial population of 7.28 log CFU/ml at time 0 in a time-course study (control). Colony-forming units were quantified on Brain-Heart Infusion Agar with 0.1% pyruvate (BHA-P). Bars represent the standard deviation of three independent samples. (b) Venn diagram showing proteins among the three iTRAQ datasets of control versus three time sampling points; T1, T2, and T3 represented 5 min, 30 min, and 1 hr sampling time-point datasets. (c) GO enrichment analysis of the time-course study of differentially expressed proteins of *L. monocytogenes* ATCC 19115 due to environmental stresses of low pH 3.5 and high water activity of a_w 0.90.

pH 3.5 and water activity of 0.900 at 25°C in a time-course study of sampling time at 5 min (mean = 6.1 log CFU/ml), 30 min (mean = 4.8 log CFU/ml), and 1 h (mean = 4.8 log CFU/ml). From the culturable count information, the inactivation happened immediately after the treatment with

the viable count dropping by an average of 1.2 log units in 5 min and 2.5 log units after 30 min after which viability remained stable when sampled at 1 h (Figure 1). The results are consistent with previous findings [16, 17] that there is a survivor population (approximately 0.3% of the original

population) following the nonthermal inactivation used; however, the size and persistent viability of this population is dependent on the temperature during the inactivation. As the temperature increases, the traits that provide protection would overcome more rapidly accelerating the inactivation process [16].

To better understand the potential mechanisms adopted by *L. monocytogenes* to respond to combined acidic and osmotic shock, the present study employed iTRAQ techniques to examine protein changes in *L. monocytogenes* for the same samples for which the culturability was determined above. The raw data were then analyzed using MASCOT, and the proteins were quantified. From the iTRAQ 4× plex experiments, a total of 1768 proteins were identified. Amongst these, 51 of the proteins generated had significantly differentiated abundance (≥ 0.5 -fold or ≤ -0.5 -fold change). A Venn diagram shows the details of the overlap between treatments and the proteins that were unique to each time dataset (Figure 1(b)). A total of 31 proteins significantly changed in abundance across all time points (5 min, 30 min, and 1 h). Enrichment analyses of these proteins based on GO terms are shown in Figure 1(c). The GO terms of level 2 associated with 18 GO categories were found for the significantly changed proteins. Eight GO term groups were derived based on biological processes and included metabolic, single-organism, and cellular processes. Six groups were derived for cell components and included mainly the whole cell and the membrane. Four derived groups were based on their molecular function and linked to catalytic activity and binding. These results suggest responses are quite global in nature affecting many aspects of the cell.

For the time-course study, bacterial cells were harvested right before the acidic and hyperosmotic treatments at time 0 and 5 min, 30 min, and 1 h after the shift, at temperature of 25°C. It also should be noted that these time points were chosen with the aim to characterize the physiology of *L. monocytogenes* during dynamic changes in viability induced by the acidic and hyperosmotic shift. Specifically, the samples taken at time 0 and 5 min were obtained during the period in which the sudden reduction of cell viability was observed, whereas the samples at time 30 min and 1 h were analyzed to determine the physiological state of *L. monocytogenes* after the sudden downshift of reduction of cell culturability. However, in Figure 2, the data for 5 min samples gave the largest number of significant proteins and then it drops away with longer incubation time likely indicating protein synthesis or turnover is occurring in only a small segment of the cell population. This also indicates the cells react to acidic and hyperosmotic downshift in a very short time with enough time to elicit some significant proteins abundance changes.

Table 1 and Figure 3 include the complete list of proteins with significant changes in the expression level at all time points. To investigate a possible interdependence of the proteins within the functional groups and to visualize their expression patterns in response to low pH and high salt stress, hierarchical clustering was performed to find associated changes of the 51 acid and salt-responsive proteins in both Table 1 and Figure 3. Three major clusters were

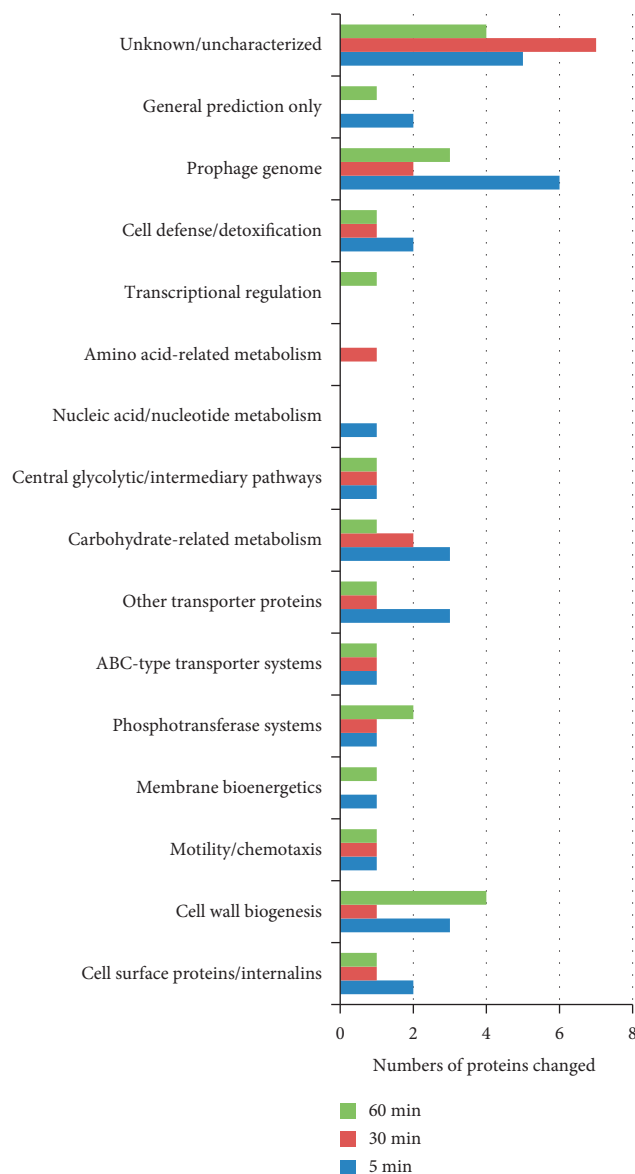


FIGURE 2: Numbers of protein changed significantly, for the log ratio of the fold change in protein abundance ≥ 0.5 or ≤ -0.5 , in each functional classes during the inactivation process in TSB-YE with pH 3.5 and a_w 0.90 with sampling time at 5 min, 30 min, and 1 hr at 25°C for a time-course study.

observed in this cluster tree (Figure 3, left). As observed from Figure 3, the number of upregulated proteins was predominant compared to those with the decreased expression level for the time-course study. The exposure of *L. monocytogenes* to simultaneous acidic and hyperosmotic shock evokes a complex response involving abundant changes of proteins of a number of functional categories (Figure 2) and metabolic pathways (Figure 4). Fewer proteins showing reduced abundance could be due to enzymes associated with protein turnover being less active. As shown in Figure 2, there are several functional categories showing more pronounced overall changes including proteins associated with prophage, cell wall biogenesis, cell defense and detoxification, carbohydrate-related metabolism, transporter

TABLE 1: Whole proteome analysis of *L. monocytogenes* ATCC 19115 responses to acidic and hyperosmotic stresses in a time-course study.

EGD-e loci	Gene name	5 min/C	Log ratio 30 min (C)	1 hr (C)	Known or predicted specific function
lmo0438	IntA	2.195	1.978	1.827	Uncharacterised protein
lmo2275		1.827	1.756	1.829	Protein gp28 [<i>Listeria monocytogenes</i> EGD-e]-[ref NP_465799.1]
lmo2834	MviM	1.799	1.333	1.562	Putative dehydrogenase, NADH dep., GFO_IDH_MocA superfamily
lmo2127	YdiL	1.689	1.329	1.77	Uncharacterised protein
lmo2135	FrwC	1.372	0.959	1.267	PTS (fructose/mannitol family) IIC-5
lmo0032	NagC	1.145	0.931	0.951	Putative glucokinase, FGGY_N superfamily
lmo2012	YesL	1.079	0.779	0.73	DUF624 superfamily protein
lmo1961	TrxB	0.865	0.925	0.872	TrxB-like thioredoxin disulfide reductase, pyr_redox superfamily
lmo0118	lmaA	0.763	0.489	0.558	Putative phage tail protein, phage_tail_2_superfamily; antigen a protein LmaA
lmo0347	DAK1	0.698	0.603	0.756	Dihydroxyacetone kinase, C-terminal domain
lmo2801	NanE	0.676	0.218	0.459	N-acetylmannosamine-6-phosphate epimerase
lmo1216	FlgJ	0.673	0.216	0.666	Exoglucosaminidase/muramidase
lmo0125	YhgE	0.671	0.356	0.459	Putative phage protein
lmo0927	MdoB	0.664	0.451	0.543	Exported glycerolphosphate lipoteichoic acid synthetase
lmo0744	LolD	0.662	0.455	0.181	Putative efflux ABC transporter, ATP-binding/permease
lmo0117		0.641	0.283	0.492	Putative phage protein; antigen B protein LmaB
lmo0724		0.635	0.341	0.388	Peptidase C39A family
lmo0412		0.629	0.486	0.461	Uncharacterised membrane-associated secreted protein
lmo2776		0.62	0.371	0.364	Putative lactococcin-like bacteriocin, lactococcin_972 superfamily
lmo0433	inlA	0.614	0.41	0.442	Internalin A; cell wall protein with LRR and B repeat domains InlA
lmo0130	UshA	0.611	0.418	0.425	Putative cell surface anchored 5'-nucleotidase
lmo2505	Spl	0.607	0.384	0.848	Peptidoglycan DL-endopeptidase P45
lmo2714		0.601	0.511	0.502	Putative cell wall sorted protein
lmo0681		0.572	0.697	0.626	Flagellar GTP-binding protein
lmo2467	FN3	0.572	0.363	0.289	Putative chitin-binding protein, chitin_bind_3/FN3/chtBD3 superfamily
lmo0186	YabE	0.555	0.31	0.582	Resuscitation-promoting factor/stationary-phase survival autolysin, Rpf/Sps_SpsB subfamily
lmo0121		0.518	0.406	0.47	Putative phage-associated membrane protein, COG5412 family
lmo0405	PitA	0.512	0.307	0.489	Low affinity phosphate transporter
lmo2849		0.487	0.666	0.381	Rhamnulokinase RhaB
lmo0768	UgpB	0.442	0.502	0.542	Hypothetical protein lmo0768 [<i>Listeria monocytogenes</i> EGD-e]-[ref NP_464295.1]
lmo1983	IlvD	0.439	0.854	0.417	Dihydroxy-acid dehydratase
lmo2132	Crp	0.424	0.446	0.53	Putative crp-like transcriptional regulator, CAP_ED superfamily
lmo2278	LysA	0.365	0.584	0.072	L-alanoyl-D-glutamate peptidase [<i>Listeria monocytogenes</i> EGD-e]-[ref NP_465802.1]
lmo2274		0.34	0.605	0.197	Protein gp30 [<i>Listeria monocytogenes</i> EGD-e]-[ref NP_465797.1]
lmo0868		0.126	1.062	0.16	Uncharacterised protein
lmo2553	AgID2	-0.06	0.081	-0.66	Integral membrane protein, COG392 superfamily
lmo2096	SgcC	-0.1	0.353	-0.51	PTS (galactitol family) IIC-2
lmo2302		-0.2	0.534	-0.69	Phage genome-associated protein
lmo2054		-0.29	-0.62	-0.09	DUF2129 superfamily protein
lmo0088	AtpE	-0.52	-0.32	-0.74	F0F1-type ATP synthase, subunit c
lmo0779	YobD	-0.52	-0.52	-0.34	Membrane protein, DUF986 superfamily
lmo1417	BtlA	-0.54	-0.35	-0.22	MFS efflux superfamily transporter
lmo2385		-0.56	-0.39	-0.56	Paal_thioesterase family protein

When *p* value is <0.01, log ratio values are in bold.

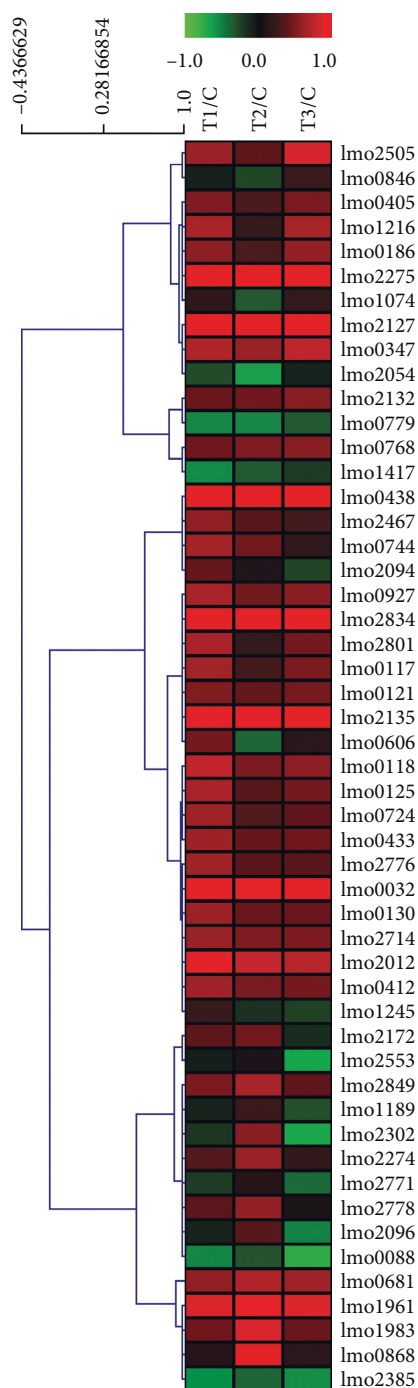


FIGURE 3: Heat map generated from proteomic data of totally 51 significantly differentially expressed proteins organized by each rows of individual proteins using hierarchical clustering. The identity of each protein can be found in Table 1. The proteins that increased and decreased in abundance are indicated in red and green, respectively. Complete linkage analysis was used to cluster biological replicate data and proteins data relative to each other. Time points T1, T2, and T3 represents 5 min, 30 min, and 1 hr cultures after the low pH (3.5) and high water activity (0.90) treatments of early stationary phase *L. monocytogenes* ATCC 19115 cells.

systems, and cell surface proteins and internalins. In the following paragraphs, proteins which have been significantly changed due to acidic and hyperosmotic shock and included

in each of the categories listed in Figure 2 will be discussed. Protein equivalent gene locus is given as the designations given for strain EGD-e (NCBI accession code NC_003210).

Proteins linked to complete or remnant prophages comprised the functional group with the highest numbers of proteins changed at 5 min exposure (Figure 2). Proteins of a conserved remnant prophage region increased in abundance at all time points including antigen B (LmaB, lmo0117), antigen A (LmaA, lmo0118), phage-related protein (lmo0121), and an YhgE superfamily protein (lmo0125). The phage A118 family protein gp28 (lmo2275) was the second most induced protein in the dataset increasing 1.83, 1.76, and 1.83 log₂-fold at 5 min, 30 min, and 1 h, respectively (Table 1 and Figure 3.). Hypothetical phage protein lmo2302 was only transiently upregulated at 30 min followed by being downregulated at 1 hr (Table 1 and Figure 3). In many *L. monocytogenes* strains, an A118 family prophage is integrated into a gene homologous to *comK* of *B. subtilis*, a regulatory transcriptional factor for competence development [37]. Acid stress has been shown to induce prophage genes in *Listeria monocytogenes* [5, 38, 39] and could be part of a mechanism where phage reproduction is activated by a sudden alteration of the cytoplasmic environment. More experiments will be needed to determine if the observed protein induction actually leads to phage reproduction or is instead part of nonspecific response to acid shock.

For cell wall biogenesis, which has the highest numbers of proteins changed at 60 min in Figure 2, FlgJ (lmo1216), MdoB (lmo0927), Spl (lmo2505), and YabE (lmo0186) were upregulated (Table 1 and Figure 3). The FlgJ paralog (lmo1216) and Spl (lmo2505) are involved in peptidoglycan turnover, with the latter protein as one of the major actors in the process [40–42]. MdoB and TagA are involved with the synthesis of lipoteichoic acid (Figure 4). The responses could be linked to cell defense related to cytoplasmic homeostasis since higher cell wall and membrane integrity and lower permeability would be advantageous for survival under the inactivation scenario studied here. Similarly, cell defenses may be nonspecifically invoked such as TrxB (lmo1961, Table 1 and Figure 3), which is a broad-spectrum thio-redoxin reductase, and thus maintains protein functionality and helps remediate an altered cytoplasmic environment through carrying out nonspecific redox reactions (Figure 4). In the general stress response and acid tolerance response stress, there is an upregulation of redox and oxidative management systems [5, 17, 43–47] in *L. monocytogenes* though the pattern of responses varies between strains and with the nature and intensity of stress exposures.

Carbohydrate metabolism and energy generation-associated proteins MviM (lmo2834), NanE (lmo2801), FN3 (lmo2467), and lmo2849 were upregulated (Table 1 and Figure 3). lmo2849 is involved in pentose interconversions, converting L-rhamnulose to L-rhamnulose-1P and L-xylulose into glycolaldehyde and glycerone-P. NanE is involved in the transformation of ManNAc-6P to GlcNAc-6. Lmo2467 homolog is a putative chitin-binding protein (Figure 4). MviM, equivalent to YcjS in *E. coli* is an uncharacterised oxidoreductase. Phosphotransferase system protein FrwC (lmo2135; [48]) was induced significantly at all

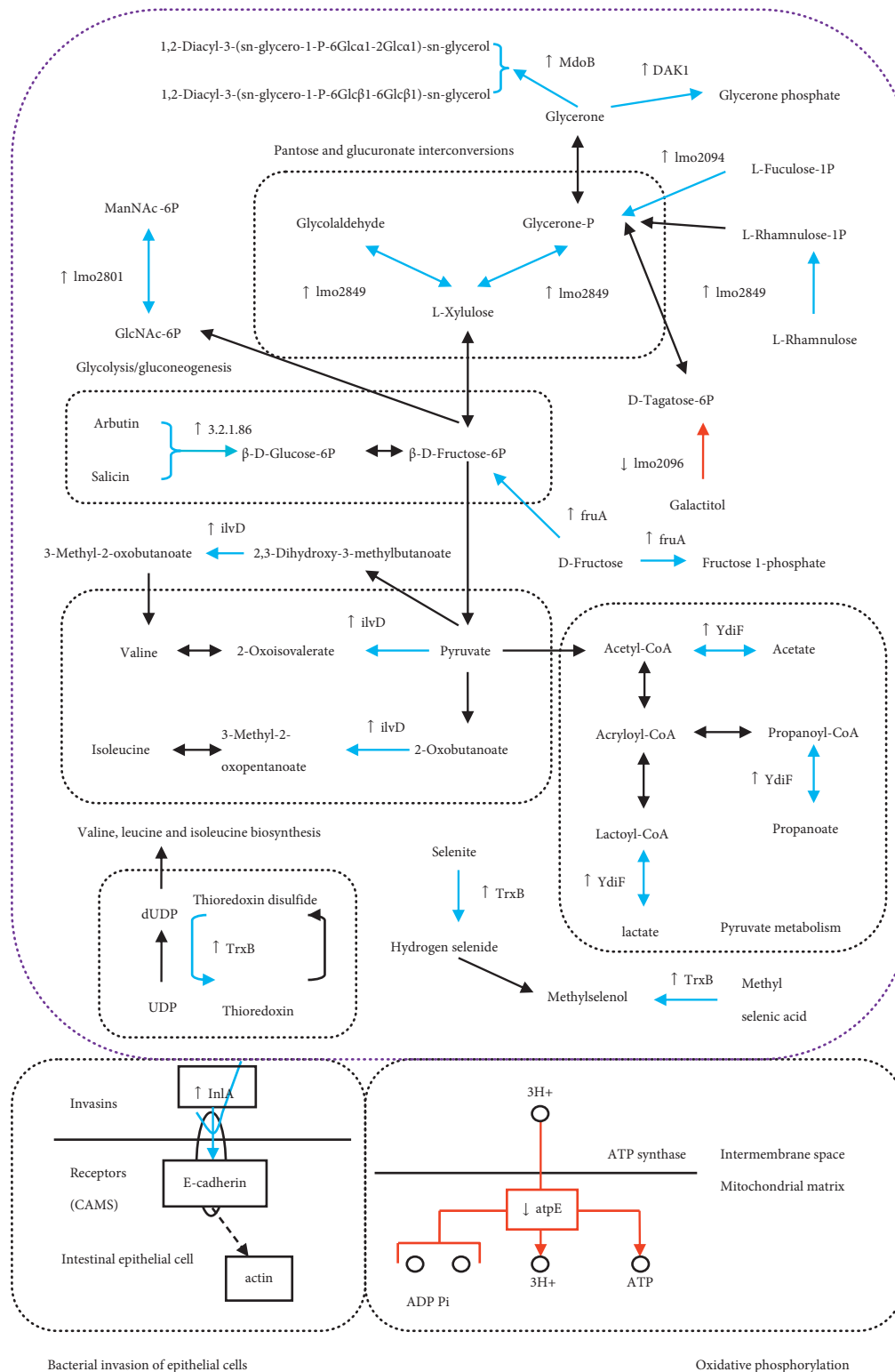


FIGURE 4: Metabolic map of intermediary metabolism of *L. monocytogenes* ATCC 19115 under nongrowth permissive acidic and hyperosmotic conditions of pH 3.5 and a_w 0.90. The map was constructed from spectral abundance data and demonstrates relative abundance of pathway components during inactivation and support data related to accumulated metabolic end-products. Pathway assignments of proteins are based on information from the KEGG database. Blue arrows indicate significant increases, and red arrows represent significant decreases in log ratio of the fold change in protein abundance proteins related to each pathway with the sampling time at 5 min, 30 min, and 1 hr at 25°C for a time-course study.

time points, while SgcC (lmo2096) was downregulated (Table 1 and Figure 3). FrwC is involved in fructose uptake, while SgcC is involved in the uptake of galactitol (dulcitol) which is subsequently converted to D-tagatose-1,6P which is then catabolised via glycolysis. NagC (lmo0032) was induced by up to 1.15, 0.93, and 0.95 log₂-fold at the analyzed time points (Table 1 and Figure 3). This protein is most likely a ROK family repressor for the adjacent carbohydrate uptake and metabolism system (lmo0033-0035) though the compounds metabolised remain largely uncharacterised [49, 50]. These could include Maillard products based on lmo0035 being a putative glucosylsine-6-phosphate deglycase. Though glycolysis stayed unchanged during stress (as has been observed previously for acid stress) [5], central glycolytic/intermediary pathways, DAK1 (lmo0347), was induced significantly at all time points. DAK1 is one of a number of paralog dihydroxyacetone kinases transforming glycerone derived from carbohydrate catabolic reactions into glycerone phosphate which then consequently enters the glycolysis pathway contributing to ATP formation (Figure 4). These responses may suggest the activation of secondary carbohydrate catabolism, which is consistent with the cell being depleted of ATP. ATP was found to be depleted from cells exposed to combined acid/salt stress, a phenomenon accelerated greatly when temperature increases. At 45°C, the rate of ATP loss is >100-fold that of 25°C and mirrors the rate of cell death [17, 18]. The uptake of utilizable carbohydrates and subsequent catabolism, either by fermentation or by oxidative reactions, is the only way this depletion can be compensated for besides general energy conservation mechanisms. Upregulation of DAK1 could be part of this response with the role to remove toxic dihydroxyacetone that would otherwise accumulate. Under the inactivation scenario, the survivor population likely has managed to achieve less ATP depletion possible due to a more intact cytoplasmic environment and higher ATP level per cell as well as better cytoplasm remediation. It was noted AtpE (lmo0088), which forms the proton channel of the secondary F1F0-ATPase complex in *L. monocytogenes*, was observed to be downregulated (Figure 4), the significance of this is unclear since it is normally weakly expressed, and one possibility is that peptides were misidentified.

The combined stress shocks were generally found to have no major effect on the expression of proteins involved in ABC-type transporter systems or other transporters requiring an intact chemiosmotic gradient to function [40, 51–53]. In this study, a LolD-like ABC-type exporter (lmo0744) was substantially upregulated (Table 1 and Figure 3), and this protein has been previously observed to be induced in *L. monocytogenes* under single-factor stress conditions (salt or acid) [5, 14, 54, 55]. UgpB (lmo0768), a multiple sugar ABC transporter substrate-binding protein used for intracellular survival, and PitA (lmo0405), a low affinity phosphate transporter, were upregulated as well. BtlA, a MFS efflux superfamily transporter (lmo1417), was downregulated. These results indicated that many transporters likely have a limited impact due to either a direct lack of ATP or by a compromised proton gradient. Specific ABC systems could allow *L. monocytogenes* cell survival by either

helping acquire utilizable energy sources to generate ATP and also possibly help remediate the cytoplasm to reattain homeostasis.

Combined stress-impacted flagella localization and induced certain virulence genes were required for surface attachment and host survival. Of motility proteins, only the flagella synthesis regulator FlhF (lmo0681) was significantly upregulated across all three time points of the time-course study (Table 1 and Figure 3). This protein controls localization of flagella through the GamR/MogR pathway and the increase could compensate for lack of flagellin units being exported. Based on this data, some cells would become sessile. The data also hints at possible beginnings of virulence induction. Cell surface proteins, InlA (lmo0433) and lmo2714, were upregulated, especially lmo2714 which was more abundant across all time points (Table 1 and Figure 3). InlA is required for adhesion and bacterial invasion of gut epithelial cells (Figure 4), while lmo2714 is a peptidoglycan bound protein that is activated during infection [56] though the exact role it has is still unknown. LntA (lmo0438) an immunomodulatory protein was the most induced protein by up to 2.20, 1.98, and 1.83 log₂-fold at all time points (Table 1 and Figure 3). LntA is a small basic protein with no sequence homology to any known protein, but it is included in a set of listerial factors that are able to reprogram host transcriptional responses in order to deregulate defense genes [57–60]. This was a surprising result and may suggest that, under particular conditions, stress rapidly activates certain aspects of virulence preparedness; however, due to the complexity of the regulatory systems (including thermoregulation) and the stationary growth phase background, only some proteins are detected.

Amino acid metabolic enzymes generally did not alter expression levels after the combined acid and osmotic shocks. For this study, IlvD (lmo1983) was found to be upregulated (Table 1 and Figure 3). IlvD catalyses the penultimate step for valine and isoleucine biosynthesis (Figure 4) and could influence branched chain fatty acid (BCFA) synthesis. BCFA have been shown to be crucial for survival of *L. monocytogenes* to adverse pH (both acidic and alkaline) and the pathways for BCFA synthesis [9]. Similarly, changes to transcriptional regulator abundance were limited, likely due to the general stress response already being invoked during transition to the stationary growth phase [5]. One transcriptional regulator, Crp (lmo2132), was upregulated (Table 1 and Figure 3); however, the exact function of this protein is unknown at present but could be linked to modulations in metabolism, a typical function for this class of protein.

Some proteins with unknown or predicted general function were activated under combined acid and salt stress. YdiL (lmo2127) was induced significantly by up to 1.69, 1.33, and 1.77 log₂-fold at all time points (Table 1 and Figure 3). Based on homology, it is a CAAX amino terminal membrane protease family protein with an at present uncharacterised function in *L. monocytogenes*. The uncharacterised DUF624 superfamily protein YesL (lmo2012) was also induced by up to 1.08, 0.78, and 0.73 log₂-fold at all time points (Table 1 and Figure 3). Likewise, the uncharacterised protein lmo2385

was also repressed across all time points (Table 1 and Figure 3). This protein belongs to PaaI thioesterase family protein. YobD (lmo0779) was downregulated and comprises a DUF986 superfamily membrane protein. Gene deletion studies are required to determine if these proteins aid survival.

3.1. Summary of Responses to Acid/Hyperosmotic Shock. Previous studies demonstrated cells that lose viability under combined acid/hyperosmotic shock tested here are effectively permanently inactivated [18]; thus, it is quite likely the responses observed are more localized in the surviving subpopulation; however, whether the degree of protein abundance changes is larger in these cells than the inactivated cell population is unknown. All of these responses can be linked to responses typical of acid stress: (1) cells could become sessile due to lack of flagellin export, which would tend to be energy conserving; (2) some aspects of carbohydrate metabolism and transport are induced to provide ATP necessary for cytoplasmic homeostasis and reactions needed to maintain cell viability; (3) some aspects of virulence—as indicated by induction of proteins InlA, lmo2714, and LntA—are increased possibly by regulatory differences between strains of *L. monocytogenes*; ATCC 19115 is a clinical 4b serotype strain and so could act as a differently typical food serotype 1/2a isolate; (4) cell envelope integrity maintenance is a priority since loss of a barrier to external protons and sodium ions would lead to rapid cytoplasmic changes and cell death; since viable subpopulations persist, this clearly suggests when cells expose to stresses, this defense functions successfully to some extent; and (5) proteins such as TrxB may help to remediate cytoplasmic proteins impacted by changes in the cytoplasmic environment due to entry of external ions. The protein abundance responses are relatively muted (usually less than 3–4-fold) which could be due to the rapid loss of cell viability, and the responses that occur are subtle only comprising parts of the many cell systems present, perhaps owing to the sensitivity limitations of the techniques used; nevertheless, the data seem largely to agree with other studies of nonthermal, in particular acidic stress, on *L. monocytogenes*. The rapid inactivation of most of the cell population challenges the ability of standard proteomic methods to capture protein information in a way that is deeply meaningful. Further investigations conducted to observe significant protein fold changes in dying cell populations could be better performed using advanced accurate proteomic methods such as SWATH (sequential window acquisition of all theoretical fragment ion spectra) which captures more information and thus allows for a deeper analysis.

4. Conclusions

The general relevance of this study to food microbiology and food quality minimal processing methods that are used to maximize food quality and that have no thermal kill step are unlikely to impact significantly on *L. monocytogenes* in terms of survival resulting in persistent supply chain risk. This

would occur either through cross-contamination or growth in the food product, especially if it is a long shelf-life chilled product. Though many processing techniques, grouped together as hurdles, can effectively hinder growth of *L. monocytogenes* sufficiently to a low risk, such as combinations of chilling, salt, and acidulants, the data presented here demonstrate that hazard reduction is still key for maximizing food safety and that new or existing methods used for food processing need to take into account the survival capability of *L. monocytogenes* and its ever-present capability of surviving even quite extreme stress.

Data Availability

The proteomics data used to support the findings of this study have been downloaded from uniprot_Listeria_96746_20150521.fasta protein repository (total of 96746 datasets).

Conflicts of Interest

The authors declare that they have no conflicts of interest.

Acknowledgments

The authors wish to thank the National Natural Science Foundation of China (grant no. 31601391), Shanghai Natural Science Foundation (grant no. 15ZR1427900), and Technology Foundation for Selected Overseas Chinese Scholar, Ministry of Human Resources and Social Security of the People's Republic of China (grant no. 2011-412) for the financial support provided to this project. The authors also thank Shanghai Hoogen Biotechnology Co. Ltd. for providing technical support.

References

- [1] J. M. Farber and P. I. Peterkin, "Listeria monocytogenes, a food-borne pathogen," *Microbiology Review*, vol. 55, no. 3, pp. 476–511, 1991.
- [2] M. Lynch, J. Painter, R. Woodruff, C. Braden, and Centers for Disease Control and Prevention, "Prevention Surveillance for foodborne-disease outbreaks—United States, 1998–2002," *Morbidity and Mortality Weekly Report. Surveillance Summaries*, vol. 55, no. 10, pp. 1–42, 2006.
- [3] P. S. Mead, L. Slutsker, V. Dietz et al., "Food-related illness and death in the United States," *Emerging Infectious Diseases*, vol. 5, no. 5, pp. 607–625, 1999.
- [4] R. Ágoston, K. Soni, P. R. Jesudhasan, W. K. Russell, C. Mohácsi-Farkas, and S. D. Pillai, "Differential expression of proteins in *Listeria monocytogenes* under thermotolerance-inducing, heat shock, and prolonged heat shock conditions," *Foodborne Pathogens and Disease*, vol. 6, no. 9, pp. 1133–1140, 2009.
- [5] J. P. Bowman, E. Hages, R. E. Nilsson, C. Kocharunchitt, and T. Ross, "Investigation of the *Listeria monocytogenes* Scott A acid tolerance response and associated physiological and phenotypic features via whole proteome analysis," *Journal of Proteome Research*, vol. 11, no. 4, pp. 2409–2426, 2012.
- [6] I. Plumbridge, L. Steil, C. Scharf, U. Volker, and E. Bremer, "Adaptation of *Bacillus subtilis* to growth at low temperature:

- a combined transcriptomic and proteomic appraisal," *Microbiology*, vol. 152, no. 3, pp. 831–853, 2006.
- [7] G. Cacace, M. F. Mazzeo, A. Sorrentino, V. Spada, A. Malorni, and R. A. Siciliano, "Proteomics for the elucidation of cold adaptation mechanisms in *Listeria monocytogenes*," *Journal of Proteomics*, vol. 73, no. 10, pp. 2021–2030, 2010.
 - [8] O. Duche, F. Tremoulet, A. Namane, and J. Labadie, "A proteomic analysis of the salt stress response of *Listeria monocytogenes*," *FEMS Microbiology Letters*, vol. 215, no. 2, pp. 183–188, 2002.
 - [9] E. S. Giotis, A. Muthaiyan, I. S. Blair, B. J. Wilkinson, and D. A. McDowell, "Genomic and proteomic analysis of the alkali-tolerance response (AlTR) in *Listeria monocytogenes* 10403S," *BMC Microbiology*, vol. 8, no. 1, p. 102, 2008.
 - [10] M. Ignatova, B. Guével, E. Com et al., "Two-dimensional fluorescence difference gel electrophoresis analysis of *Listeria monocytogenes* submitted to a redox shock," *Journal of Proteomics*, vol. 79, pp. 13–27, 2013.
 - [11] L. Phan-Thanh and T. Gormon, "Stress proteins in *Listeria monocytogenes*," *Electrophoresis*, vol. 18, no. 8, pp. 1464–1471, 1997.
 - [12] S. L. Salscheider, A. Jahn, and K. Schnetz, "Transcriptional regulation by BglJ–RcsB, a pleiotropic heteromeric activator in *Escherichia coli*," *Nucleic Acids Research*, vol. 42, no. 5, pp. 2999–3008, 2014.
 - [13] H. Bierne and P. Cossart, "When bacteria target the nucleus: the emerging family of nucleomodulins," *Cellular Microbiology*, vol. 14, no. 5, pp. 622–633, 2012.
 - [14] J. R. Pittman, J. O. Buntyn, G. Posadas, B. Nanduri, K. Pendarvis, and J. R. Donaldson, "Proteomic analysis of cross protection provided between cold and osmotic stress in *Listeria monocytogenes*," *Journal of Proteome Research*, vol. 13, no. 4, pp. 1896–1904, 2014.
 - [15] M. Gandhi and M. L. Chikindas, "*Listeria*: a foodborne pathogen that knows how to survive," *International Journal of Food Microbiology*, vol. 113, no. 1, pp. 1–15, 2007.
 - [16] T. Ross, D. Zhang, and O. J. McQuestin, "Temperature governs the inactivation rate of vegetative bacteria under growth-preventing conditions," *International Journal of Food Microbiology*, vol. 128, no. 1, pp. 129–135, 2008.
 - [17] D. Zhang, O. J. McQuestin, L. A. Mellefont, and T. Ross, "The influence of non-lethal temperature on the rate of inactivation of vegetative bacteria in inimical environments may be independent of bacterial species," *Food Microbiology*, vol. 27, no. 4, pp. 453–459, 2010.
 - [18] D. L. Zhang, T. Ross, and J. P. Bowman, "Physiological aspects of *Listeria monocytogenes* during inactivation accelerated by mild temperatures and otherwise non-growth permissive acidic and hyperosmotic conditions," *International Journal of Food Microbiology*, vol. 141, no. 3, pp. 177–185, 2010.
 - [19] Y. Zhu, H. Xu, H. Chen et al., "Proteomic analysis of solid pseudopapillary tumor of the pancreas reveals dysfunction of the endoplasmic reticulum protein processing pathway," *Molecular & Cellular Proteomics*, vol. 13, no. 10, pp. 2593–2603, 2014.
 - [20] J. R. Wisniewski, A. Zougman, N. Nagaraj, and M. Mann, "Universal sample preparation method for proteome analysis," *Nature Methods*, vol. 6, no. 5, pp. 359–362, 2009.
 - [21] M. Ashburner, C. A. Ball, J. A. Blake et al., "Gene ontology: tool for the unification of biology," *Nature Genetics*, vol. 25, no. 1, pp. 25–29, 2000.
 - [22] S. Gotz, J. M. Garcia-Gomez, J. Terol et al., "High-throughput functional annotation and data mining with the Blast2GO suite," *Nucleic Acids Research*, vol. 36, no. 10, pp. 3420–3435, 2008.
 - [23] M. Kanehisa, S. Goto, Y. Sato, M. Furumichi, and M. Tanabe, "KEGG for integration and interpretation of large-scale molecular data sets," *Nucleic Acids Research*, vol. 40, no. D1, pp. D109–D114, 2012.
 - [24] E. C. Friedberg, G. C. Walker, W. Siede, R. D. Wood, R. A. Schultz, and T. Ellenberger, *DNA Repair and Mutagenesis*, ASM Press, Washington, DC, USA, 2nd edition, 2006.
 - [25] J. D. Helmann, M. F. W. Wu, P. A. Kobel et al., "Global transcriptional response of *Bacillus subtilis* to heat shock," *Journal of Bacteriology*, vol. 183, no. 24, pp. 7318–7328, 2001.
 - [26] E. Henke and U. Bornscheuer, "Esterases from *Bacillus subtilis* and *B. stearothermophilus* share high sequence homology but differ substantially in their properties," *Applied Microbiology and Biotechnology*, vol. 60, no. 3, pp. 320–326, 2002.
 - [27] A. Petersohn, M. Brigulla, S. Haas, J. D. Hoheisel, U. Volker, and M. Hecker, "Global analysis of the general stress response of *Bacillus subtilis*," *Journal of Bacteriology*, vol. 183, no. 19, pp. 5617–5631, 2001.
 - [28] E. Quevillon, V. Silventoinen, S. Pillai et al., "InterProScan: protein domains identifier," *Nucleic Acids Research*, vol. 33, pp. W116–W120, 2005.
 - [29] F. Cairrão, A. Cruz, H. Mori, and C. M. Arraiano, "Cold shock induction of RNase R and its role in the maturation of the quality control mediator SsrA/tmRNA," *Molecular Microbiology*, vol. 50, no. 4, pp. 1349–1360, 2003.
 - [30] C. Chen and M. P. Deutscher, "Elevation of RNase R in response to multiple stress conditions," *Journal of Biological Chemistry*, vol. 280, no. 41, pp. 34393–34396, 2005.
 - [31] L. He, Q.-L. Deng, M.-t. Chen, Q.-p. Wu, and Y.-J. Lu, "Proteomics analysis of *Listeria monocytogenes* ATCC 19115 in response to simultaneous triple stresses," *Archives of Microbiology*, vol. 197, no. 6, pp. 833–841, 2015.
 - [32] F. Kunst, N. Ogasawara, I. Moszer et al., "The complete genome sequence of the gram-positive bacterium *Bacillus subtilis*," *Nature*, vol. 390, no. 6657, pp. 249–256, 1997.
 - [33] A. Lebreton, P. Cossart, and H. Bierne, "Bacteria tune interferon responses by playing with chromatin," *Virulence*, vol. 3, no. 1, pp. 87–91, 2012.
 - [34] J. Melo, P. W. Andrew, and M. L. Faleiro, "Different assembly of acid and salt tolerance response in two dairy *Listeria monocytogenes* wild strains," *Archives of Microbiology*, vol. 195, no. 5, pp. 339–348, 2013.
 - [35] C. W. Price, P. Fawcett, H. Cérémonie, N. Su, C. K. Murphy, and P. Youngman, "Genome-wide analysis of the general stress response in *Bacillus subtilis*," *Molecular Microbiology*, vol. 41, no. 4, pp. 757–774, 2002.
 - [36] J.-H. Shin and C. W. Price, "The SsrA-SmpB ribosome rescue system is important for growth of *Bacillus subtilis* at low and high temperatures," *Journal of Bacteriology*, vol. 189, no. 10, pp. 3729–3737, 2007.
 - [37] M. J. Loessner, R. B. Inman, P. Lauer, and R. Calendar, "Complete nucleotide sequence, molecular analysis and genome structure of bacteriophage A118 of *Listeria monocytogenes*: implications for phage evolution," *Molecular Microbiology*, vol. 35, no. 2, pp. 324–340, 2000.
 - [38] G. Ercoli, C. Tani, A. Pezzicoli et al., "LytM proteins play a crucial role in cell separation, outer membrane composition, and pathogenesis in nontypeable *Haemophilus influenzae*," *mBio*, vol. 6, no. 2, 2015.
 - [39] T. Uehara, T. Dinh, and T. G. Bernhardt, "LytM-domain factors are required for daughter cell separation and rapid

- ampicillin-induced lysis in *Escherichia coli*,” *Journal of Bacteriology*, vol. 191, no. 16, pp. 5094–5107, 2009.
- [40] P. Cabrita, M. J. Trigo, R. B. Ferreira, and L. Brito, “Is the exoproteome important for bacterial pathogenesis? Lessons learned from Interstrain exoprotein diversity in *Listeria monocytogenes* grown at different temperatures,” *OMICS: A Journal of Integrative Biology*, vol. 18, no. 9, pp. 553–569, 2014.
 - [41] S. K. Singh, L. SaiSree, R. N. Amrutha, and M. Reddy, “Three redundant murein endopeptidases catalyse an essential cleavage step in peptidoglycan synthesis of *Escherichia coli* K12,” *Molecular Microbiology*, vol. 86, no. 5, pp. 1036–1051, 2012.
 - [42] T. Uehara, K. R. Parzych, T. Dinh, and T. G. Bernhardt, “Daughter cell separation is controlled by cytokinetic ring-activated cell wall hydrolysis,” *EMBO Journal*, vol. 29, no. 8, pp. 1412–1422, 2010.
 - [43] J. M. Aramini, S. Sharma, Y. J. Huang et al., “Solution NMR structure of the SOS response protein YnzC from *Bacillus subtilis*,” *Proteins: Structure, Function, and Bioinformatics*, vol. 72, no. 1, pp. 526–530, 2008.
 - [44] N. Au, E. Kuester-Schoeck, V. Mandava et al., “Genetic composition of the *Bacillus subtilis* SOS system,” *Journal of Bacteriology*, vol. 187, no. 22, pp. 7655–7666, 2005.
 - [45] A. R. Fernandez de Henestrosa, T. Ogi, S. Aoyagi et al., “Identification of additional genes belonging to the LexA regulon in *Escherichia coli*,” *Molecular Microbiology*, vol. 35, no. 6, pp. 1560–1572, 2002.
 - [46] Y. Kawai, S. Moriya, and N. Ogasawara, “Identification of a protein, YneA, responsible for cell division suppression during the SOS response in *Bacillus subtilis*,” *Molecular Microbiology*, vol. 47, no. 4, pp. 1113–1122, 2003.
 - [47] W. L. Kelley, “Lex marks the spot: the virulent side of SOS and a closer look at the LexA regulon,” *Molecular Microbiology*, vol. 62, no. 5, pp. 1228–1238, 2006.
 - [48] J. Plumbridge, “Regulation of PTS gene expression by the homologous transcriptional regulators, Mlc and NagC, in *Escherichia coli*,” *Journal of Molecular Microbiology and Biotechnology*, vol. 3, pp. 371–380, 2001.
 - [49] D. Bréchemier-Baey, L. Domínguez-Ramírez, J. Oberto, and J. Plumbridge, “Operator recognition by the ROK transcription factor family members, NagC and Mlc,” *Nucleic Acids Research*, vol. 43, no. 1, pp. 361–372, 2015.
 - [50] M. D. Kazanov, X. Li, M. S. Gelfand, A. L. Osterman, and D. A. Rodionov, “Functional diversification of ROK-family transcriptional regulators of sugar catabolism in the Thermotogae phylum,” *Nucleic Acids Research*, vol. 41, no. 2, pp. 790–803, 2013.
 - [51] C. G. M. Gahan, J. O’Mahony, and C. Hill, “Characterization of the groESL operon in *Listeria monocytogenes*: utilization of two reporter systems (gfp and hly) for evaluating in vivo expression,” *Infection and Immunity*, vol. 69, no. 6, pp. 3924–3932, 2001.
 - [52] P. M. Jones and A. M. George, “The ABC transporter structure and mechanism: perspectives on recent research,” *Cellular and Molecular Life Sciences (CMLS)*, vol. 61, no. 6, pp. 682–699, 2004.
 - [53] G. Segal and E. Z. Ron, “Regulation and organization of the groE and dnaK operons in Eubacteria,” *FEMS Microbiology Letters*, vol. 138, no. 1, pp. 1–10, 1996.
 - [54] E. Borezee, E. Pellegrini, and P. Berche, “OppA of *Listeria monocytogenes*, an oligopeptide-binding protein required for bacterial growth at low temperature and involved in intracellular survival,” *Infection and Immunity*, vol. 68, no. 12, pp. 7069–7077, 2000.
 - [55] G. M. Dunny and B. A. B. Leonard, “Cell-cell communication in gram-positive bacteria,” *Annual Review of Microbiology*, vol. 51, no. 1, pp. 527–564, 1997.
 - [56] A. Camejo, C. Buchrieser, E. Couvé et al., “In vivo transcriptional profiling of *Listeria monocytogenes* and mutagenesis identify new virulence factors involved in infection,” *PLoS Pathogens*, vol. 5, no. 5, article e1000449, 2009.
 - [57] H. Bierne, M. Hamon, and P. Cossart, “Epigenetics and bacterial infections,” *Cold Spring Harbor Perspectives in Medicine*, vol. 2, no. 12, article a010272, 2012.
 - [58] M. A. Hamon, E. Batsche, B. Regnault et al., “Histone modifications induced by a family of bacterial toxins,” *Proceedings of the National Academy of Sciences*, vol. 104, no. 33, pp. 13467–13472, 2007.
 - [59] A. Lebreton, G. Lakisic, V. Job et al., “A bacterial protein targets the BAHDI chromatin complex to stimulate type III interferon response,” *Science*, vol. 331, no. 6022, pp. 1319–1321, 2011.
 - [60] F. Titgemeyer, J. Reizer, A. Reizer, and M. H. Saier, “Evolutionary relationships between sugar kinases and transcriptional repressors in bacteria,” *Microbiology*, vol. 140, no. 9, pp. 2349–2354, 1994.

